Monthly Notices
of the
ROYAL ASTRONOMICAL SOCIETY

MNRAS **475,** L81–L85 (2018)
Advance Access publication 2018 January 12

doi:10.1093/mnrasl/sly010

Accurate effective temperatures of the metal-poor benchmark stars HD 140283, HD 122563, and HD 103095 from CHARA interferometry

I. Karovicova,[1★] T. R. White,[2★] T. Nordlander,[3] K. Lind,[4,5★] L. Casagrande,[3] M. J. Ireland,[3] D. Huber,[2,6,7,8] O. Creevey,[9] D. Mourard,[9] G. H. Schaefer,[10] G. Gilmore,[11] A. Chiavassa,[9] M. Wittkowski,[12] P. Jofré,[13] U. Heiter,[5] F. Thévenin[9] and M. Asplund[3]

[1]*Zentrum für Astronomie der Universität Heidelberg, Landessternwarte, Königstuhl 12, D-69117 Heidelberg, Germany*
[2]*Department of Physics and Astronomy, Stellar Astrophysics Centre, Aarhus University, Ny Munkegade 120, DK-8000 Aarhus C, Denmark*
[3]*Research School of Astronomy & Astrophysics, Australian National University, Canberra, ACT 2611, Australia*
[4]*Max Planck Institute für Astronomy, Königstuhl, D-69117 Heidelberg, Germany*
[5]*Observational Astrophysics, Department of Physics and Astronomy, Uppsala University, Box 516, SE-75120 Uppsala, Sweden*
[6]*Institute for Astronomy, University of Hawai'i, 2680 Woodlawn Drive, Honolulu, HI 96822, USA*
[7]*Sydney Institute for Astronomy (SIfA), School of Physics, University of Sydney, NSW 2006, Australia*
[8]*SETI Institute, 189 Bernardo Avenue, Mountain View, CA 94043, USA*
[9]*Université de La Côte d'Azur, OCA, Laboratoire Lagrange CNRS, BP. 4229, F-06304 Nice Cedex, France*
[10]*Department of Physics and Astronomy, Georgia State University, PO Box 5060, Atlanta, GA 30302-5060, USA*
[11]*Institute of Astronomy, University of Cambridge, Madingley Road, Cambridge CB3 0HA, UK*
[12]*European Southern Observatory, Karl-Schwarzschild-Str. 2, D-85748 Garching bei München, Germany*
[13]*Núcleo de Astronomía, Universidad Diego Portales, Av. Ejército 441, Santiago, Chile*

Accepted 2018 January 8. Received 2017 December 29; in original form 2017 November 27

ABSTRACT

Large stellar surveys of the Milky Way require validation with reference to a set of 'benchmark' stars whose fundamental properties are well determined. For metal-poor benchmark stars, disagreement between spectroscopic and interferometric effective temperatures has called the reliability of the temperature scale into question. We present new interferometric measurements of three metal-poor benchmark stars, HD 140283, HD 122563, and HD 103095, from which we determine their effective temperatures. The angular sizes of all the stars were determined from observations with the PAVO beam combiner at visible wavelengths at the CHARA array, with additional observations of HD 103095 made with the VEGA instrument, also at the CHARA array. Together with photometrically derived bolometric fluxes, the angular diameters give a direct measurement of the effective temperature. For HD 140283, we find $\theta_{\rm LD} = 0.324 \pm 0.005$ mas, $T_{\rm eff} = 5787 \pm 48$ K; for HD 122563, $\theta_{\rm LD} = 0.926 \pm 0.011$ mas, $T_{\rm eff} = 4636 \pm 37$ K; and for HD 103095, $\theta_{\rm LD} = 0.595 \pm 0.007$ mas, $T_{\rm eff} = 5140 \pm 49$ K. Our temperatures for HD 140283 and HD 103095 are hotter than the previous interferometric measurements by 253 and 322 K, respectively. We find good agreement between our temperatures and recent spectroscopic and photometric estimates. We conclude some previous interferometric measurements have been affected by systematic uncertainties larger than their quoted errors.

Key words: standards – techniques: interferometric – surveys – stars: individual: HD 103095 – stars: individual: HD 122563 – stars: individual: HD 140283.

1 INTRODUCTION

Understanding the stellar populations of the Galaxy relies upon precise determination of fundamental stellar properties. One of the main challenges in the determination of global parameters of stars is an accurate estimate of the effective temperature, $T_{\rm eff}$. Temperatures are commonly derived from spectroscopy or photometry, however, neither of these techniques provide a direct determination of this parameter. The most direct and, in comparison to spectroscopy or photometry, nearly model-independent measurements of $T_{\rm eff}$ come from the combination of interferometric measurements of the angular

★ E-mail: karovicova@uni-heidelberg.de (IK); timw@phys.au.dk (TRW); klind@mpia.de (KL)

diameter, θ, with a determination of the bolometric flux, $F_{\rm bol}$, given by

$$T_{\rm eff} = \left(\frac{4F_{\rm bol}}{\sigma\theta^2}\right)^{1/4}, \quad (1)$$

where σ is the Stefan–Boltzmann constant.

Current observational constraints limit precise interferometric measurements of the angular diameter θ to relatively bright ($V < 8$ mag) stars with $\theta \gtrsim 0.3$ mas. Consequently, measurements are limited to only a few metal-poor stars, typically close to these limits. In particular, angular diameters have been measured by Creevey et al. (2012, 2015) for the brightest and most nearby metal-poor G-type subgiant HD 140283, K-type red giant branch star HD 122563, and K-type dwarf HD 103095. However, some differences have been found between interferometric temperatures and those derived from spectroscopy and photometry that are difficult to reconcile, particularly for HD 140283 and HD 103095 (see Heiter et al. 2015, and references therein for a detailed discussion). Heiter et al. (2015) recommended that both these stars should not be used as temperature standards until these differences can be resolved.

As these stars are currently the only metal-poor benchmark stars (Jofré et al. 2014; Heiter et al. 2015) selected for the large stellar survey conducted by the *Gaia* mission (Gaia Collaboration et al. 2016) as well as the supporting *Gaia*-ESO spectroscopic survey (Gilmore et al. 2012; Randich, Gilmore & Gaia-ESO Consortium 2013), and are used as standard stars in a large number of spectroscopic studies, it is of the utmost importance that these issues are resolved. In this study, we therefore present new interferometric observations at visible wavelengths of these three metal-poor stars.

2 OBSERVATIONS

2.1 Interferometric observations and data reduction

We observed the three stars using the PAVO beam combiner at the CHARA array at Mt. Wilson Observatory, California (ten Brummelaar et al. 2005). PAVO is a pupil-plane beam combiner operating between ∼600 and 900 nm, with a spectral dispersion of each scan typically producing visibility measurements in 27 independent wavelength channels (Ireland et al. 2008). The limiting magnitude of the PAVO instrument is $R \sim 7.5$ mag (8 mag in ideal conditions). We observed the stars using baselines between 156.3 and 313.6 m. The stars were observed between 2014 April 8 and 2017 June 16. We also obtained VEGA (Mourard et al. 2009) observations of HD103095 in 2017 March and May. VEGA is a dispersed fringes beam combiner. For these observations, we defined a spectral band of 15 or 20 nm wide, around the central wavelength of the observations (either 700 or 720 nm). Our observations are summarized in Table 1.

The raw data were reduced using the PAVO reduction software, which has been well tested and used in multiple studies (Bazot et al. 2011; Derekas et al. 2011; Huber et al. 2012; Maestro et al. 2013). To monitor the interferometric transfer function, we observed a set of calibration stars. Calibrators, selected from the *Hipparcos* catalogue (ESA 1997), were chosen to be likely unresolved sources and located close on the sky to the science target. Calibrators were observed immediately before and after the science target. The angular diameters of the calibrators were determined using the *V*–*K* relation of Boyajian, van Belle & von Braun (2014) and corrected for limb-darkening (LD) to determine the uniform disc diameter in *R* band. We use *V*-band magnitudes from the Tycho-2 catalogue (Høg et al. 2000) converted into the Johnson system using the calibration by Bessell (2000), and *K*-band magnitudes from the Two Micron All Sky Survey (2MASS; Skrutskie et al. 2006). We use the dust map of Green et al. (2015) to estimate the reddening, and adopt the reddening law of O'Donnell (1994). The diameter for the VEGA calibrator is obtained from the JMMC Stellar Diameters Catalog (JSDC; Chelli et al. 2016). Details of the calibrators are summarized in Table 2. The calibrated squared visibility measurements of our three targets are shown in Fig. 1 as a function of spatial frequency.

HD 140283 is a particularly difficult target to observe due to its small size, southern declination, and it being relatively faint. The observations made during 2017 were particularly challenging due to a temporarily reduced sensitivity of the CHARA Array while an adaptive optics system was installed and not yet operational. While the 2017 observations display an increased scatter in visibility, the measured diameter is consistent across all observing seasons.

Table 1. Log of interferometric observations.

HD	UT date	Combiner	Baseline[a]	Scans	Cal.[b]
140283	2014 Apr 8	PAVO	E1W1	4	jkl
	2015 Apr 4	PAVO	S1W1	2	jk
	2017 June 16	PAVO	E1W1	4	ik
122563	2017 Mar 3	PAVO	E2W2	3	ehi
	2017 June 9	PAVO	E2W2	2	gi
	2017 June 10	PAVO	E2W2	2	fi
103095	2015 May 2	PAVO	E2W2	3	ab
	2017 Mar 3	PAVO	E2W2	3	ad
		PAVO	E2W1	2	ad
	2017 Mar 4	PAVO	E1W2	3	abd
	2017 Mar 13	VEGA	W1W2	3	c
	2017 Mar 14	VEGA	W1W2	3	c
	2017 May 5	VEGA	S2W2	3	c

Notes. [a]The baselines used have the following lengths: W1W2, 107.93 m; E2W2, 156.27 m; S2W2, 177.45 m; E1W2, 221.85 m; E2W1, 251.34 m; S1W1, 278.50 m; E1W1, 313.57 m. [b]Refer to Table 2 for details of the calibrators used.

Table 2. Calibrator stars used for interferometric observations.

HD	Sp. T.	V (mag)	K (mag)	$E(B-V)$ (mag)	$\theta_{\rm UD,R}$ (mas)	ID
99002	F0	6.93	6.28	0.008	0.201(10)	a
103288	F0	7.00	6.22	0.006	0.211(11)	b
103928	A9V	6.42	5.60	0.002	0.282(7)	c
107053	A5V	6.68	6.02	0.004	0.226(11)	d
120448	A0	6.78	6.52	0.017	0.169(8)	e
120934	A1V	6.10	5.96	0.007	0.216(11)	f
121996	A0Vs	5.76	5.70	0.029	0.238(12)	g
122365	A2V	5.98	5.70	0.007	0.248(12)	h
128481	A0	6.98	6.79	0.007	0.149(7)	i
139909	B9.5V	6.86	6.54	0.110	0.165(8)	j
143259	B9V	6.64	6.28	0.107	0.187(9)	k
146214	A1V	7.49	7.10	0.012	0.132(7)	l

2.2 Modelling of limb-darkened angular diameters

Resolving a small-scale structure, such as LD, requires measurements in the sidelobes of the visibility function. The low contrast of the interference fringes in the sidelobes and the need for the star to be overresolved limit such measurements to bright stars with large angular sizes (e.g. Kervella et al. 2017). Our measurements are therefore degenerate between a uniformly illuminated disc and

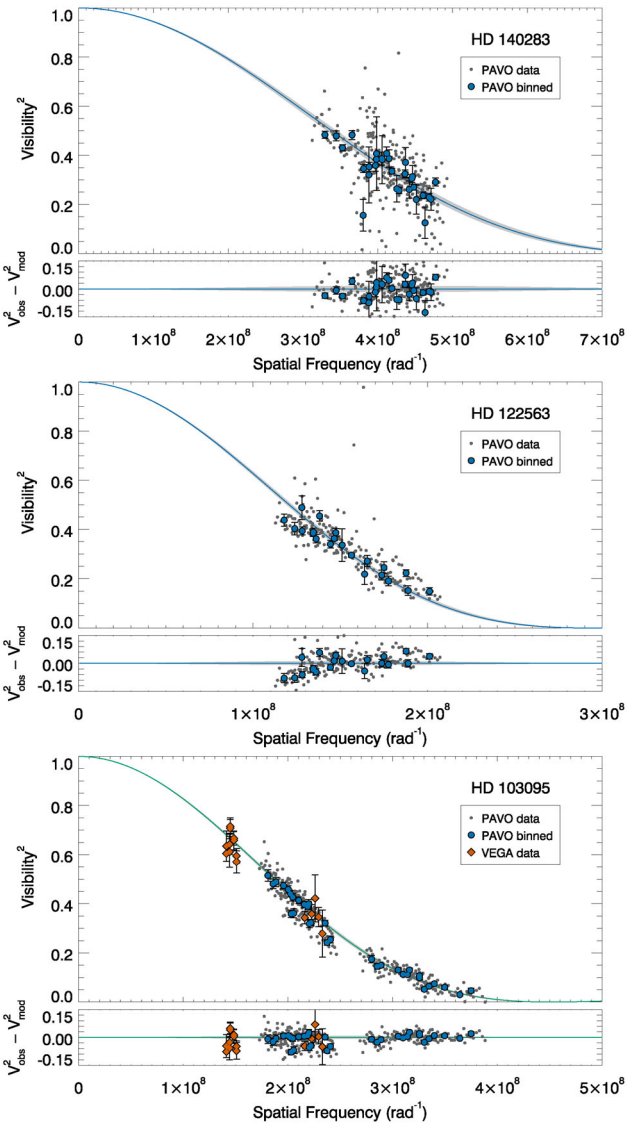

Figure 1. Squared visibility versus spatial frequency for HD 140283, HD 122563, and HD 103095. The grey points are PAVO measurements. For clarity, we show weighted averages of the PAVO measurements over nine wavelength channels as blue circles. The blue line shows the fitted limb-darkened model to the PAVO data, with the light grey-shaded region indicating the 1σ uncertainties. For HD 103095, measurements were also made with the VEGA beam combiner (orange diamonds), with the best-fitting model to the combined data indicated by the green line. The lower panels show the residuals from the fit.

a limb-darkened disc. Input from stellar model atmospheres is required to determine an appropriate amount of LD to infer the true angular diameters of these stars. LD laws, which parametrize the intensity variation with a small number of coefficients, are commonly employed, with grids of coefficients calculated for various model atmospheres, LD laws, and photometric filters (e.g. Claret & Bloemen 2011).

The use of the linear LD law is ubiquitous in interferometric studies due to its simple form and the ease with which different studies can be compared. However, it has long been known that the linear law does not fully describe the intensity distribution across the stellar disc in either observations or models (e.g. Klinglesmith & Sobieski 1970), and higher order LD laws have been developed. To achieve a more faithful representation of the model atmosphere, we used a four-term non-linear LD law (Claret 2000). For ease of comparison to other interferometric studies, we have also fitted each star with a uniform disc model and a linearly limb-darkened disc model.

For a generalized polynomial LD law,

$$\frac{I(\mu)}{I(1)} = \sum_k c_k \mu^k, \tag{2}$$

with $\mu = \cos\gamma$, and γ is the angle between the line of sight and the emergent intensity, the visibility is given by (Quirrenbach et al. 1996)

$$V(x) = \left[\sum_k \frac{c_k}{k+2}\right]^{-1} \sum_k c_k 2^{k/2} \Gamma\left(\frac{k}{2}+1\right) \frac{J_{k/2+1}(x)}{x^{(k/2+1)}}, \tag{3}$$

where $x = \pi B \theta \lambda^{-1}$, with B the projected baseline, θ the angular diameter, and λ the wavelength of observation, $\Gamma(z)$ is the gamma function, and $J_n(x)$ is the nth-order Bessel function of the first kind. The quantity $B\lambda^{-1}$ is the spatial frequency.

LD coefficients in the R band were determined from LD tables computed by Magic et al. (2015) from the STAGGER-grid, a set of state-of-the art 3D radiation-hydrodynamical model atmospheres that are computed from first principles. We generated initial values of the LD coefficients by interpolating the grid of coefficients to the spectroscopic atmospheric parameters adopted from the literature (Bergemann et al. 2012; Ramírez, Allende Prieto & Lambert 2013; Bensby, Feltzing & Oey 2014). For HD 140283, the initial values were $T_{\rm eff} = 5658$ K, $\log(g) = 3.6$, and [Fe/H] $= -2.62$ dex; for HD 122563, they were $T_{\rm eff} = 4665 \pm 80$ K, $\log(g) = 1.64 \pm 0.16$, and [Fe/H] $= -2.51$ dex; for HD 103095, they were $T_{\rm eff} = 5149 \pm 70$ K, $\log(g) = 4.71 \pm 0.3$, and [Fe/H] $= -1.27 \pm 0.2$ dex. We estimate uncertainties $T_{{\rm eff},\sigma} = 90$ K, $\log(g)_\sigma = 0.3$, and [Fe/H]$_\sigma = 0.2$. The influence on LD coefficients from deviations from the initial spectroscopic values is negligible.

Uncertainties in the spectroscopic parameters were used to generate 10 000 realizations of the LD coefficients to estimate their uncertainties, and, in the case of the four-term law, their correlations. Additionally, we determined 1D LD coefficients based on Claret & Bloemen (2011) using the same spectroscopic values as for the 3D simulations (Table 3). The results based on 1D and 3D models are consistent within the uncertainties and the uncertainties are in both cases similar. We used both 1D and 3D modelling for comparison, however, the 3D simulations are important for a complete characterization of the stellar surface properties. The 3D-based LD is better supported by the observed solar centre-to-limb variation (Pereira et al. 2013) and exoplanet transit light curves (Hayek et al. 2012). Further details will be given in a following paper (Karovicova et al., in preparation).

The fit to the interferometric measurements was performed following the procedure described by Derekas et al. (2011), estimating angular diameter uncertainties by performing Monte Carlo simulations that take into account the uncertainties in the visibility measurements, wavelength calibration (0.5 per cent), calibrator sizes, and the LD coefficients. For HD 103095, we performed fits to the PAVO and VEGA data, both separately and combined.

The new interferometric $T_{\rm eff}$ was calculated using the derived angular diameter and bolometric flux (see Section 2.3). The LD coefficients were then redetermined using the new $T_{\rm eff}$, with the process iterated until the results converged. The final angular diameter measurements are listed in Table 3, and the fits of the 3D limb-darkened diameters are shown in Fig. 1.

Table 3. Angular diameters and LD coefficients.

Star	Combiner	θ_{UD} (mas)	Linear LD[a]		Four-term LD[a]				
			u	θ_{LD} (mas)	a_1	a_2	a_3	a_4	θ_{LD} (mas)
HD 140283	PAVO	0.312 ± 0.006	0.550 ± 0.009	0.327 ± 0.005	1.62 ± 0.11	-2.11 ± 0.30	2.01 ± 0.32	-0.68 ± 0.12	0.324 ± 0.005
HD 122563	PAVO	0.882 ± 0.010	0.632 ± 0.006	0.937 ± 0.011	1.26 ± 0.09	-1.20 ± 0.13	1.25 ± 0.13	-0.43 ± 0.05	0.926 ± 0.011
HD 103095	PAVO	0.565 ± 0.005	0.631 ± 0.008	0.601 ± 0.005	0.49 ± 0.11	0.51 ± 0.14	-0.30 ± 0.12	0.06 ± 0.05	0.595 ± 0.007
	VEGA	0.582 ± 0.008		0.617 ± 0.009					0.611 ± 0.009
	PAVO+VEGA	0.566 ± 0.005		0.602 ± 0.005					0.596 ± 0.007

Note. [a]LD coefficients derived from the grid of Magic et al. (2015); see the text for details.

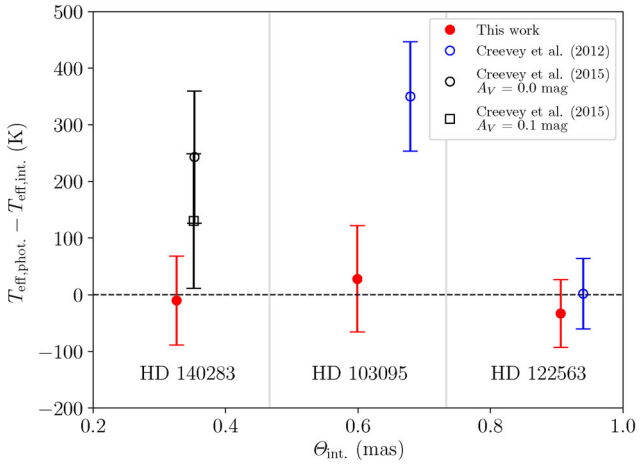

Figure 2. Filled red circles are effective temperatures $T_{\rm eff,phot} - T_{\rm eff,int.}$ versus interferometric measurements. $T_{\rm eff,phot}$ Casagrande et al. (2010) for HD 140283, Casagrande et al. (2014) for HD 122563, and Casagrande et al. (2011) for HD 103095. Blue open circles represent measurements from Creevey et al. (2012) for HD 103095 and HD 122563, and black open symbols from Creevey et al. (2015) a circle for HD 140283 and an open square for $A_V = 0.1$ mag.

2.3 Bolometric flux

Bolometric fluxes for HD 140283 and HD 122563 were derived using the InfraRed Flux Method (IRFM) as described in Casagrande et al. (2010, 2014). Only HD 140283 has 2MASS photometry of sufficiently high quality for this implementation of the IRFM, although for HD 122563 we circumvented the problem by converting Johnson *JHK* photometry into the 2MASS system.[1] The IRFM depends very mildly on the adopted log (g) and [Fe/H] of the stars. We iterated the IRFM with spectroscopic parameters until reaching convergence in bolometric fluxes. For HD 103095, we used bolometric corrections in the Tycho2 $B_T V_T$ and *Hipparcos* H_p system from Casagrande & VandenBerg (2014). For this star, bolometric corrections were computed at the spectroscopic $T_{\rm eff}$, log (g), and [Fe/H]. We remark that the effective temperatures we derive from the IRFM, as well as the adopted spectroscopic $T_{\rm eff}$ for HD 103095, are all in agreement with interferometric ones to within a few tens of degrees at most (Fig. 2). We adopted a reddening of zero for both HD 103095 and HD 140283 because of their vicinity, ∼10 and 60 pc, respectively, and hence within the local bubble (e.g. Leroy 1993; Lallement et al. 2003). Interstellar Na I D lines confirm the absence of reddening for HD 140283 (Meléndez et al. 2010). HD 122563 is the only star showing non-zero reddening, and we adopt $E(B-V) = 0.003$ mag, following Creevey et al. (2012) and consistent with our preliminary analysis of interstellar Na I D lines (Karovicova et al., in preparation). A considerable higher value such as $E(B-V) = 0.01$ mag for this star would increase the bolometric flux by 1 per cent, which is well within our adopted uncertainties.

[1] http://www.astro.caltech.edu/~jmc/2mass/v3/transformations where Johnson has been converted using the 2MASS-Bessell & Brett.

3 RESULTS AND DISCUSSION

Our updated fundamental stellar parameters of the three metal-poor benchmark stars are given in Table 4. Both the uncertainty in the angular diameter and the bolometric flux contribute significantly to the final uncertainty in the effective temperature. For HD 140283, the angular diameter contributes ∼75 per cent, for HD 122563 they both contribute ∼50 per cent, and for HD 103095 the bolometric flux contributes ∼70 per cent.

Our angular diameters for HD 140283 and HD 103095 are smaller than those determined in previous interferometric studies of these stars (Creevey et al. 2012, 2015). For HD 103095, our measurements with VEGA imply a slightly larger diameter (0.611 ± 0.009 mas) than is obtained from our PAVO measurements (0.595 ± 0.007 mas), however both are substantially smaller than previously obtained with the FLUOR and Classic beam combiners at the CHARA array (0.679 ± 0.015 mas).

As a consequence of the smaller diameters, the inferred effective temperatures of these stars are higher. For HD 140283, it is 253 K (140 K assuming non-negligible reddening $A_V = 0.1$ mag) higher, and for HD 103095, $T_{\rm eff}$ is 322 K higher, bringing the interferometric values into better agreement with spectroscopy and photometry. HD 122563 is in a good agreement. In Fig. 2, we show the difference between recent photometric temperatures determined by Casagrande et al. (2010, 2011, 2014) and interferometric measurements presented here and by Creevey et al. (2012, 2015).

The differences between our angular diameters and those determined by Creevey et al. (2012, 2015) may be the result of systematic errors arising from the notoriously difficult calibration of interferometric observations. The system response of the interferometer is determined by measuring calibrator stars. However, errors in the

Table 4. Observed (θ_{LD}) and derived ($F_{\rm bol}$, $T_{\rm eff}$, L, R) stellar parameters.

Parameters	HD 140283	HD 122563	HD 103095
m_V (mag)	7.21	6.19	6.45
m_R (mag)	6.63	5.37	5.80
π (mas)	17.15 ± 0.14^a	4.22 ± 0.35^b	109.99 ± 0.41^b
$F_{\rm bol}$ (erg s^{-1} cm^{-2} 10^{-8})	3.93 ± 0.05	13.20 ± 0.29	8.22 ± 0.25
θ_{LD} (mas)	0.324 ± 0.005	0.926 ± 0.011	0.595 ± 0.007
$T_{\rm eff}$ (K)	5787 ± 48	4636 ± 37	5140 ± 49
L ($L_\odot$)	4.82 ± 0.27	232 ± 37	0.21 ± 0.01
R ($R_\odot$)	2.04 ± 0.04	23.7 ± 2.0	0.586 ± 0.007

Notes. [a]Bond et al. (2013)
[b]van Leeuwen (2007)

predicted size of calibrators and atmospheric variability can lead to poor estimates of the system visibility. In an effort to minimize this, we observed multiple calibrators that were as small and as close as possible to the target over several observations on different nights.

Comparisons between photometric and interferometric temperatures have noted that diameters measured in the K' band with the Classic beam combiner at the CHARA array with sizes $\lesssim$1 mas appear to be systematically larger than expected (Casagrande et al. 2014). This disagreement tends to increase with decreasing angular size, suggesting that systematic errors arise for near-infrared observations when the stars are underresolved. The differences we see with the previous measurements of these metal-poor benchmark stars are in the same direction and of similar magnitude to those noted by Casagrande et al. (2014), suggesting we are seeing the same systematic effect. By comparison, our temperatures are consistent with those determined photometrically, as shown in Fig. 2. Our observations at visible wavelengths allow us a greater resolution to avoid these systematic errors. Some of the observations of HD 103095 and HD 122563 analysed by Creevey et al. (2012) were CHARA Classic K'-band measurements, which may have contributed to the differences with our results.

The results presented here, in resolving the differences between the interferometric, spectroscopic, and photometric temperatures of these important stars, now allow for their reliable use as benchmark stars for calibrating large stellar surveys.

ACKNOWLEDGEMENTS

IK acknowledges support by the Deutsche Forschungsgemeinschaft, DFG project number KA4055 and by the European Science Foundation – GREAT *Gaia* Research for European Astronomy Training. This work was supported by Sonderforschungsbereich SFB 881 'The Milky Way System' (subproject A3) of the DFG. This work is based upon observations obtained with the Georgia State University Center for High Angular Resolution Astronomy Array at Mount Wilson Observatory. The CHARA array is supported by the National Science Foundation under Grants no. AST-1211929 and AST-1411654. Institutional support has been provided from the GSU College of Arts and Sciences and the GSU Office of the Vice President for Research and Economic Development. Funding for the Stellar Astrophysics Centre is provided by The Danish National Research Foundation. TRW acknowledges the support of the Villum Foundation (research grant 10118). MA, TN, LC, and DH gratefully acknowledge support from the Australian Research Council (grants DP150100250, FT160100402, and DE140101364, respectfully). DH also acknowledges support from the National Aeronautics and Space Administration under Grant NNX14AB92G issued through the Kepler Participating Scientist Program. GG acknowledges ERC grant 320360. KL acknowledges funds from the Alexander von Humboldt Foundation in the framework of the Sofja Kovalevskaja Award endowed by the Federal Ministry of Education and Research as well as funds from the Swedish Research Council (Grant *nr*.2015 − 00415_3) and Marie Sklodowska Curie Actions (Cofund Project INCA 600398). UH acknowledges support from the Swedish National Space Board (SNSB/Rymdstyrelsen).

REFERENCES

Bazot M. et al., 2011, A&A, 526, L4
Bensby T., Feltzing S., Oey M. S., 2014, A&A, 562, A71
Bergemann M., Lind K., Collet R., Magic Z., Asplund M., 2012, MNRAS, 427, 27
Bessell M. S., 2000, PASP, 112, 961
Bond H. E., Nelan E. P., VandenBerg D. A., Schaefer G. H., Harmer D., 2013, ApJ, 765, L12
Boyajian T. S., van Belle G., von Braun K., 2014, AJ, 147, 47
Casagrande L., VandenBerg D. A., 2014, MNRAS, 444, 392
Casagrande L., Ramírez I., Meléndez J., Bessell M., Asplund M., 2010, A&A, 512, A54
Casagrande L. S., Schönrich R., Asplund M., Cassisi S., Ramírez I., Meléndez J., Bensby T., Feltzing S., 2011, A&A, 530, A138
Casagrande L. et al., 2014, MNRAS, 439, 2060
Chelli A., Duvert G., Bourgès L., Mella G., Lafrasse S., Bonneau D., Chesneau O., 2016, A&A, 589, A112
Claret A., 2000, A&A, 363, 1081
Claret A., Bloemen S., 2011, A&A, 529, A75
Creevey O. L. et al., 2012, A&A, 545, A17
Creevey O. L. et al., 2015, A&A, 575, A26
Derekas A. et al., 2011, Science, 332, 216
ESA 1997, ESA SP-1200: The Hipparcos and Tycho catalogues. ESA, Noordwijk
Gaia Collaboration et al., 2016, A&A, 595, A1
Gilmore G. et al., 2012, The Messenger, 147, 25
Green G. M. et al., 2015, ApJ, 810, 25
Hayek W., Sing D., Pont F., Asplund M., 2012, A&A, 539, A102
Heiter U., Jofré P., Gustafsson B., Korn A. J., Soubiran C., Thévenin F., 2015, A&A, 582, A49
Huber D. et al., 2012, ApJ, 760, 32
Høg E. et al., 2000, A&A, 355, L27
Ireland M. J. et al., 2008, in Schöller M., Danchi W. C., Delplancke F., eds, Optical and Infrared Interferometry. SPIE, Bellingham, p. 701324
Jofré P. et al., 2014, A&A, 564, A133
Kervella P., Bigot L., Gallenne A., Thévenin F., 2017, A&A, 597, A137
Klinglesmith D. A., Sobieski S., 1970, AJ, 75, 175
Lallement R., Welsh B. Y., Vergely J. L., Crifo F., Sfeir D., 2003, A&A, 411, 447
Leroy J. L., 1993, A&A, 274, 203
Maestro V. et al., 2013, MNRAS, 434, 1321
Magic Z., Chiavassa A., Collet R., Asplund M., 2015, A&A, 573, A90
Meléndez J., Casagrande L., Ramírez I., Asplund M., Schuster W. J., 2010, in Charbonnel C., Tosi M., Primas F., Chiappini C., eds, Proc. IAU Symp. 268, Light Elements in the Universe. Kluwer, Dordrecht, p. 211
Mourard D. et al., 2009, A&A, 508, 1073
O'Donnell J. E., 1994, ApJ, 422, 158
Pereira T. M. D., Asplund M., Collet R., Thaler I., Trampedach R., Leenaarts J., 2013, A&A, 554, A118
Quirrenbach A., Mozurkewich D., Buscher D. F., Hummel C. A., Armstrong J. T., 1996, A&A, 312, 160
Ramírez I., Allende Prieto C., Lambert D. L., 2013, ApJ, 764, 78
Randich S., Gilmore G., Gaia-ESO Consortium, 2013, The Messenger, 154, 47
Skrutskie M. F. et al., 2006, AJ, 131, 1163
ten Brummelaar T. A. et al., 2005, ApJ, 628, 453
van Leeuwen F., 2007, A&A, 474, 653

This paper has been typeset from a TEX/LATEX file prepared by the author.